19. Balsam LB, Wagers AJ, Christensen JL, Kofidis T, Weissman IL, Robbins RC. Haematopoietic stem cells adopt mature haematopoietic fates in ischaemic myocardium. Nature 2004;428:668–73.
20. Murry CE, Wiseman RW, Schwartz SM, Hauschka SD. Skeletal myoblast transplantation for repair of myocardial necrosis. J Clin Invest 1996;98:2512–23.
21. Taylor DA, Atkins BZ, Hungspreugs P, Jones TR, Reedy MC, Hutcheson KA, et al. Regenerating functional myocardium: improved performance after skeletal myoblast transplantation. Nat Med 1998;4:929–33.
22. Menasché P. Current status and future prospects for cell transplantation to prevent congestive heart failure. Semin Thorac Cardiovasc Surg 2008;20:131–7.
23. Farahmand P, Lai TY, Weisel RD, Fazel S, Yau T, Menasche P, et al. Skeletal myoblasts preserve remote matrix architecture and global function when implanted early or late after coronary ligation into infarcted or remote myocardium. Circulation 2008;118(14 suppl):S130–7.
24. Tambara K, Sakakibara Y, Sakaguchi G, Lu F, Premaratne GU, Lin X, et al. Transplanted skeletal myoblasts can fully replace the infarcted myocardium when they survive in the host in large numbers. Circulation 2003;108(suppl 1):II259–63.

Novel regenerative therapy using cell-sheet covered with omentum flap delivers a huge number of cells in a porcine myocardial infarction model

Yasuhiro Shudo, MD,[a] Shigeru Miyagawa, MD, PhD,[a] Satsuki Fukushima, MD, PhD,[a] Atsuhiro Saito, PhD,[a] Tatsuya Shimizu, MD, PhD,[b] Teruo Okano, PhD,[b] and Yoshiki Sawa, MD, PhD[a]

Objective: A key challenge to applying cell transplantation to treat severely damaged myocardium is in delivering large numbers of cells with minimum cell loss. We developed a new implantation method using skeletal myoblast (SMB) sheets, wrapped with an omentum flap as a blood supply to deliver huge numbers of SMBs to the damaged heart. We examined whether this method could be used to deliver a large amount of cells to deteriorated porcine myocardium.

Methods: Cell sheets were obtained by culturing mini-pig autologous SMB cells on temperature-responsive culture dishes. Myocardial infarction was induced by placing an ameroid constrictor around the left anterior descending artery. The mini-pigs were divided into 4 treatment groups (n = 6 in each): cell sheets with omentum, cell sheets only, omentum only, and sham operation. Each animal implant consisted of 30 cell sheets (1.5×10^7 cells per sheet). Six 5-layer constructs were each placed on a different area, immediately adjacent to but not overlapping one another, to cover the infarct and border regions.

Results: The new regenerative cell delivery system using SMB sheets covered and wrapped with omentum resulted in (1) a significantly reduced infarct size causing, at least in part, a thin scar with thick well-vascularized cardiac tissue; (2) increased angiogenesis, as determined by a significantly higher vascular density; and (3) improved cardiac function, as determined by echocardiography, compared with the conventional method (SMB sheet implantation).

Conclusions: This cell delivery system shows potential for repairing the severely failed heart. (J Thorac Cardiovasc Surg 2011;142:1188-96)

ETVBS

Heart failure is a frequent and life-threatening disorder, despite recent medical and surgical advances. Myocardial regenerative therapy is gaining interest as a means for improving left ventricular (LV) function in patients with end-stage heart disease.[1-3] However, a recent clinical trial of cell transplantation by needle injection reported slightly disappointing results.[2-4] The main drawbacks of cell transplantation by needle injection appear to be poor retention and survival of the injected cells, local mechanical myocardial damage owing to injury by the needle itself, and the potential for lethal arrhythmias. We have been investigating cell-sheet techniques for delivering cells to severely damaged myocardium more efficiently, without damaging the myocardium, and, consequently, more effectively. This technique provides better improvement of cardiac function than obtained with the needle cell-injection method.[5-7]

The greatest advantage of the cell-sheet technique is that the sheet consists only of cells, which produce an extracellular matrix without requiring an artificial scaffold. The cell sheet has a high ability to integrate with native tissues, because the adhesion molecules on its surface are preserved.[5-7] The layered grafts must be carefully prepared to avoid tearing, but they themselves are strong, flexible, and easy to work with.

It has been suggested that an increased number of implanted skeletal myoblast (SMB) sheets is related to better results, such as improved cardiac function and angiogenesis, less fibrosis, and less hypertrophy, with the amounts of secreted cytokines dependent on the number of cell sheets used.[7] However, cell sheets with more than 5 layers show areas with disorganized vasculature, presumably because of insufficient supplies of blood, oxygen, and nutritients.[7,8] Thus, in applying cell transplantation to the severely damaged myocardium, a key challenge is in improving the blood perfusion of the implanted cells so

From the Department of Cardiovascular Surgery,[a] Osaka University Graduate School of Medicine, Suita, Osaka, Japan; and the Institute of Advanced Biomedical Engineering and Science,[b] Tokyo Women's Medical University, Tokyo, Japan.

Supported by Grants for the Research and Development of the Myocardial Regeneration Medicine Program from the New Energy Industrial Technology Development Organization (NEDO), Japan.

Disclosures: Authors have nothing to disclose with regard to commercial support.

Read at the 91st Annual Meeting of The American Association for Thoracic Surgery, Philadelphia, Pennsylvania, May 7-11, 2011.

Received for publication April 28, 2011; revisions received June 23, 2011; accepted for publication July 11, 2011; available ahead of print Sept 16, 2011.

Address for reprints: Yoshiki Sawa, MD, PhD, Department of Cardiovascular Surgery, Osaka University Graduate School of Medicine, Osaka, Japan (E-mail: sawa-p@surg1.med.osaka-u.ac.jp).

0022-5223/$36.00

doi:10.1016/j.jtcvs.2011.07.002

Abbreviations and Acronyms

LAD = left anterior descending coronary artery
LV = left ventricular
LVEDV = left ventricular end-diastolic volume
LVEF = left ventricular ejection fraction
LVESV = left ventricular end-systolic volume
MI = myocardial infarction
O group = omentum only
RT-PCR = real-time polymerase chain reaction
S group = cell sheets only
SMB = skeletal myoblast
SO group = cell sheets wrapped with omentum
STAT3 = signal transducer and activator of transcription 3
VEGF = vascular endothelial growth factor

that large numbers of regenerative cells can be delivered with minimal cell loss.

The omentum is reported to potentially provide revascularization for the ischemic myocardium,[9] release a number of angiogenic cytokines,[10,11] supply stem cells, and attenuate inflammation.[12] The omentum was once commonly used in surgical revascularization to treat ischemic heart disease; however, omentopexy alone is not very effective for supporting the angiogenesis needed in the infarcted area for rapid recovery.[9] On the basis of those findings, we speculated combining SMB sheets with omentum might enhance survival of the implanted cells by improving angiogenesis. Thus, as a novel method for implanting large amounts of cells, we developed a cell-delivery system using SMB sheets wrapped and covered with omentum flap as an external source for blood flow. We hypothesized that this method could replace the myocardial infarction (MI) scar with cell-sheet–based cardiac tissue in the pig heart.

MATERIALS AND METHODS

All studies were performed with the approval of the institutional ethics committee of Osaka University. Humane animal care was used in compliance with the "Principles of Laboratory Animal Care" formulated by the National Society for Medical Research and the "Guide for the Care and Use of Laboratory Animals" prepared by the Institute of Animal Resources and published by the National Institutes of Health (Publication No 85-23, revised 1996). The authors had full access to the data and take full responsibility for its integrity. All the authors have read and agreed to the manuscript as written. All procedures and evaluations, including the assessment of cardiac parameters, were carried out in a blinded manner.

Animal Models and Study Protocol (Figure 1)

Thirty-seven female mini-pigs (8-10 months old; Japan Farm Co Ltd, Kagoshima, Japan) weighing 20 to 25 kg were used in these experiments.

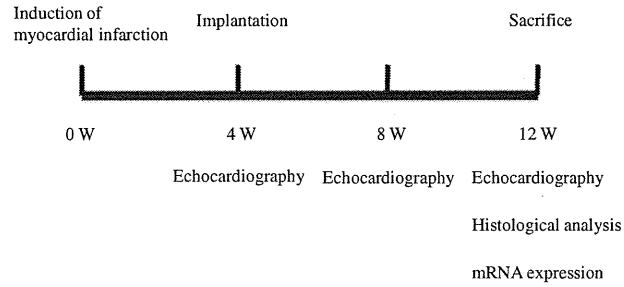

FIGURE 1. Study protocol for the assessment of cardiac function and histologic analysis.

The mini-pigs were anesthetized with an intravenous administration of ketamine (6 mg/kg) and sodium pentobarbital (10 mg/kg) for endotracheal intubation and then maintained with inhaled sevoflurane (15%-2%). The pericardial space was exposed by left thoracotomy through the fourth intercostal space. The distal portion of the left anterior descending coronary artery (LAD) was directly ligated as ischemic preconditioning to reduce the occurrence of lethal ventricular arrhythmia, followed by placement of an ameroid constrictor around the LAD just distal to the left circumflex coronary artery branching.[5,13] The muscle and skin were closed in layers, and the mini-pigs were then taken off the anesthetics. Eleven (30%) of the study animals died in the early postoperative period. This technique produced an ischemic cardiomyopathy model that reflected clinical relevance and can be used for appropriate preclinical studies with minimal procedure-related mortality.

Computer-generated random allocation generated 4 randomized study groups 1 week after MI. Autologous cells were isolated and grown in culture for 3 weeks to prepare samples for implantation. Four weeks after MI induction, the mini-pigs were again placed under general anesthesia for echocardiography followed by either cell-sheet implantation or a sham operation. Two mini-pigs whose LV ejection fractions (LVEFs) were above 40% before treatment, as measured by transthoracic echocardiography using the Simpson method, were excluded from the study. At 4 and 8 weeks after either cell-sheet implantation or sham operation, the mini-pigs again underwent general anesthesia for echocardiographic examination. The mini-pigs were humanely killed after the 8-week echocardiography measurements for histologic and biochemical analyses of the heart tissue.

Preparation and Grafting of SMB Cell Sheets

Autologous skeletal muscle weighing approximately 10 to 15 g was removed from the quadriceps femoris muscle, and purified autologous SMB cells were cultured for 3 weeks to prepare them for implantation, as described previsously.[5] Autologous SMBs are precursor cells of adult myofibers and feature several advantages, including autologous origin, high in vitro scalability, lack of tumorigenicity (owing to their myogenic lineage restriction), and strong resistance to hypoxia after ischemia. The cells were incubated in 60-mm temperature-responsive culture dishes (UpCell; Cellseed, Tokyo, Japan) at 37°C for 24 hours (1.5×10^7 cells per dish). The dishes were then transferred to another incubator, set at 20°C, for 1 hour to release the cultured cells as intact cell sheets. Under this protocol, the SMBs spontaneously detached from the plate as a free-floating monolayer cell sheet.

Grafting the SMB Cell Sheet Wrapped With Omentum

The mini-pigs with MI were divided into 4 treatment groups (n = 6 in each): cell sheets wrapped with omentum (SO group), cell sheets only (S group), omentum only (O group), and sham operation (sham group). Each animal in the SO and S groups received approximately 30 cell sheets (1.5×10^7 cells per sheet) with the total cell number being 4.5×10^8.

In the S group, a median sternotomy was performed. The cell sheets were placed on the epicardium of the ischemic area (LAD region) and stitched in place around the edge. In the SO group, a small upper midline laparotomy and median sternotomy were performed to move omentum from the peritoneal space into the mediastinal space, preserving the arch structure of the left gastroepiploic artery. We created a hole in the diaphragm and passed the omentum flap through the hole into the pericardial cavity. Five-layer cell sheets of SMBs were wrapped with omentum and then covered with the harvested omental flap, because a maximum of 5 cell-sheet layers can be implanted in one place.[7,8] Six 5-layer constructs were each placed on a different area to cover the infarct and border regions. The operations were performed with the animals under general anesthesia.

Histologic and Immunohistochemical Analyses

Eight weeks after the treatment, the hearts were dissected and embedded in optimum cutting temperature compound, snap-frozen in liquid nitrogen, and cut into 5-μm thick sections. The paraffin-embedded sections were fixed in 4% paraformaldehyde and stained with hematoxylin–eosin (Figure 2) or Masson trichrome (Figure 3). The percentage of infarct area was quantified as the positively stained LV area/total LV area. The stained and total LV areas were obtained by tracing using Image J software at the mid-LV level, where the base of the papillary muscles is clearly depicted.

So that vascular density could be evaluated in the border area, the cryosectioned samples were immunolabeled with anti–von Willebrand factor antibody (1:250 dilution; Dako, Glostrup, Denmark) (Figure 4). The number of positively stained capillary vessels that were 5 to 10 μm in diameter in the peri-infarct border-zone myocardium in 16 individual randomly selected fields per heart was counted under high-power magnification (×200). The numbers from the 16 fields were averaged to determine the vascular density (per square millimeter). The stained slides were viewed on a BioZero laser scanning microscope (Keyence, Osaka, Japan).

The following antibodies were used to identify SMBs: the primary antibodies were anti-smooth muscle actin, anti-vimentin, anti-desmin, and anti-skeletal myosin (fast) (all from Dako); the secondary antibodies were goat anti-mouse and anti-rabbit immunoglobulin G (Invitrogen, Leek, The Netherlands).

Analysis of mRNA Expression

Total RNA was extracted from cardiac muscle tissue, reverse transcribed into cDNA using TaqMan reverse transcription reagents (Applied Biosystems, Stockholm, Sweden), and real-time polymerase chain reaction (RT-PCR) was performed with an ABI PRISM 7700 machine (Applied Biosystems).[14] For each gene, RNA samples were prepared and assayed in triplicate. RT-PCR was used to determine the expressions of vascular endothelial growth factor (VEGF) and signal transducer and activator of transcription 3 (STAT3) in our in vivo experiments. The average copy number of gene transcripts for each sample was normalized to that for glyceraldehyde-3-phosphate dehydrogenase.

Echocardiography: Measurements of Global LV Function

Global cardiac function was assessed using commercially available echocardiographic equipment with a 4.0-MHz transducer (Aplio; Toshiba, Otawara, Japan) before and 4 and 8 weeks after cell-sheet implantation. Echocardiographic measurements included LV end-diastolic and end-systolic volumes (LVEDV and LVESV, respectively) and LVEF. LVEF was calculated as follows: $\text{LVEF}\,(\%) = 100 \times (\text{LVEDV} - \text{LVESV})/(\text{LVEDV})$.

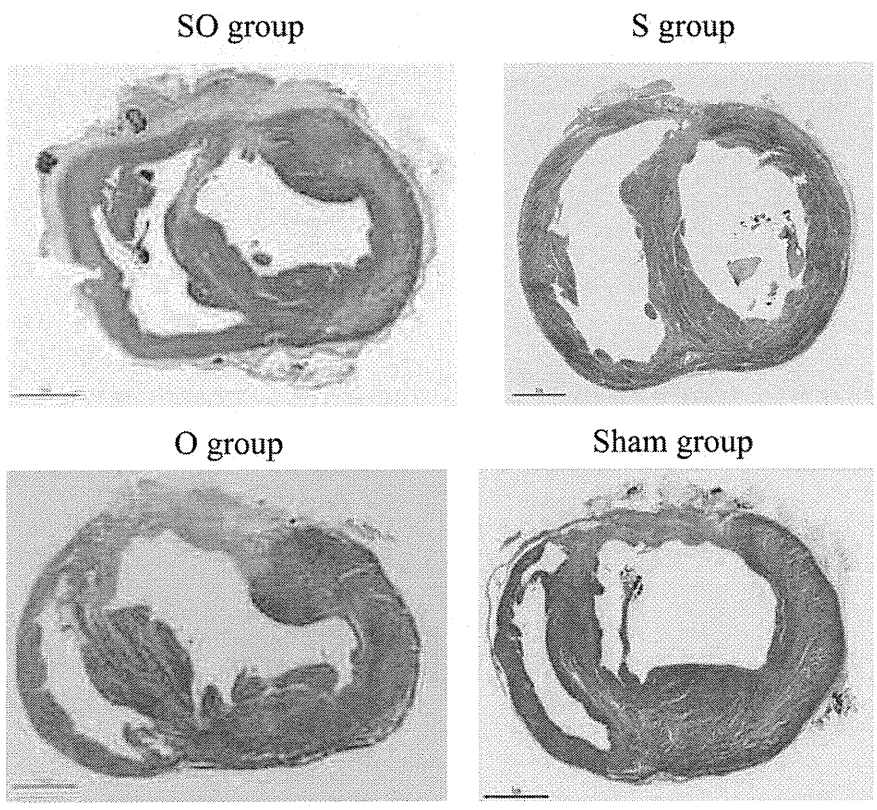

FIGURE 2. Macroscopic (×40) views of the heart in the 4 groups (hematoxylin–eosin staining). *SO group,* skeletal myoblast (SMB) sheets wrapped with omentum; *S group,* SMB sheets only; *O group,* omentum only; *sham group,* sham operation.

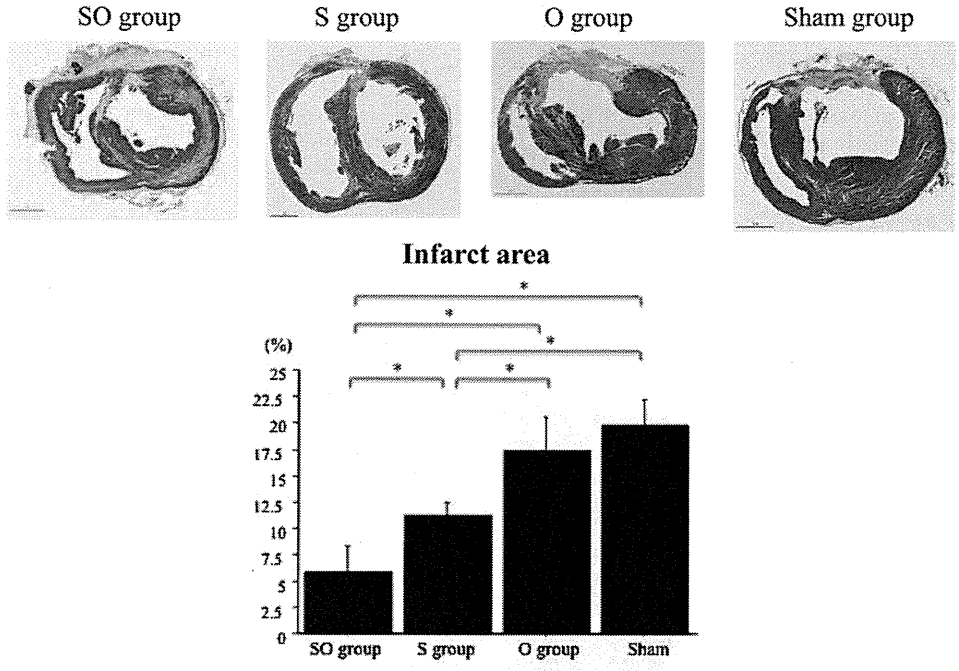

FIGURE 3. Macroscopic (×40) views of the heart in the 4 groups (Masson trichrome staining). Infarct area: The SO group showed a significant improvement in the infarct area of the whole heart. Abbreviations as in Figure 2. *$P < .05$.

Statistical Analysis

SPSS software (version 11.0, SPSS, Inc, Chicago, Ill) was used for statistical analyses. Continuous values are expressed as the mean ± standard deviation. The significance of differences was determined using a 2-tailed multiple *t* test with Bonferroni correction following analysis of variance for individual differences.

RESULTS

Modulation of Myocardial Structure

Myocardial structural components, including fibrosis and vascularity, were assessed by hematoxylin–eosin staining, Masson trichrome staining, and immunohistochemistry

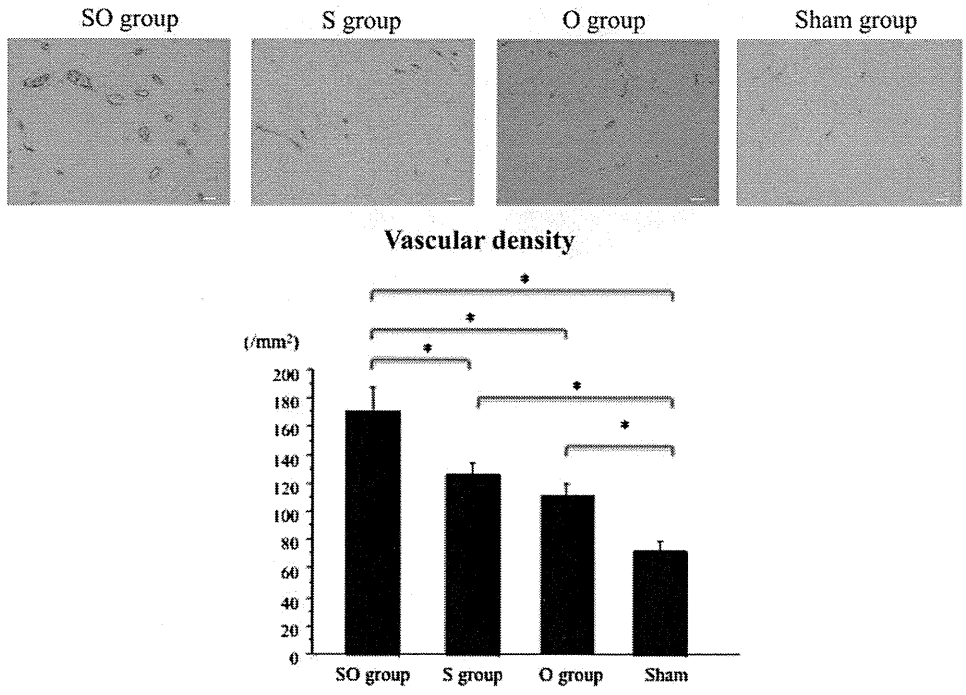

FIGURE 4. Microscopic (×200) views of sections of the peri-infarct border-zone region stained with the von Willebrand factor antibody (factor VIII) in the 4 groups (*bar* = 20 μm). Vascular density: The SO group showed a significant improvement in vascular density, as assessed by anti–von Willebrand factor antibody. Abbreviations as Figure 2. N > 4 in each group. *$P < .05$.

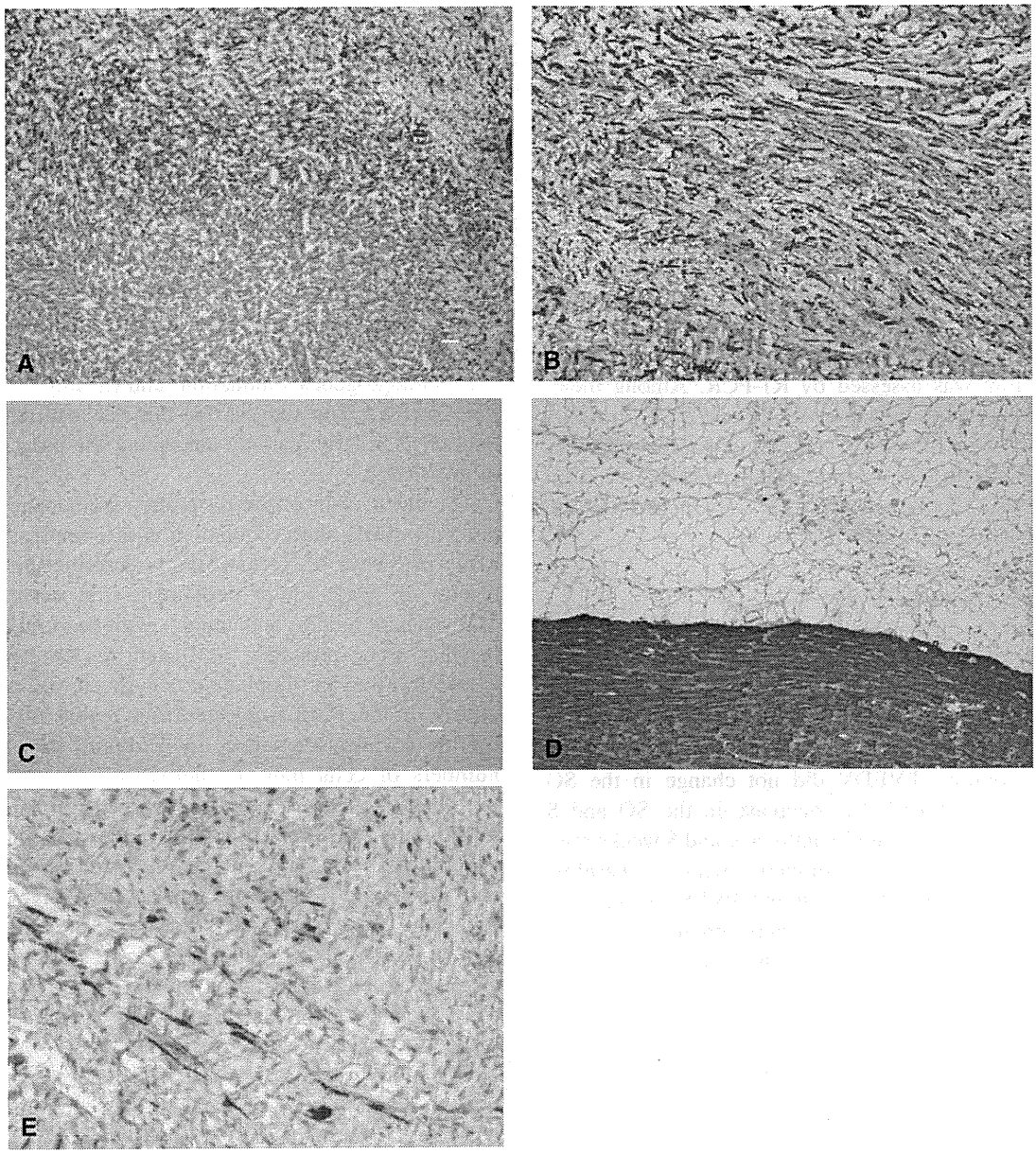

FIGURE 5. A, Microscopic (×200) views of the infarct region in the SO group (alpha smooth muscle actin staining). B, Microscopic (×200) views of the infarct region in the SO group (vimentin staining). C, Microscopic (×200) views of the infarct region in the SO group (fast type myosin heavy chain staining). D and E, Microscopic (×200) views of the heart (desmin staining). *SO group,* SMB sheets wrapped with omentum.

for anti–von Willebrand factor 8 weeks after treatment. The cavity of the LV was enlarged in the O and sham groups, whereas the global myocardial structure was well maintained in the SO and S groups, as assessed by hematoxylin–eosin staining (Figure 2). Collagen was densely accumulated in the infarct area and globally distributed in the remote area after the sham operation, whereas less collagen had accumulated in both the infarct and remote areas in the other 3 groups compared with the sham group, as assessed by Masson trichrome staining. The size of the infarct area, quantitatively assessed by computer-based planimetry of Masson trichrome–stained hearts, was significantly smaller in the SO group than in the other 3 groups (Figure 3). The vascular density, assessed by immunohistochemistry for anti–von Willebrand factor, was significantly greater in the SO group than in the other 3 groups (Figure 4).

Many alpha-smooth muscle actin- and vimentin-positive cells were present in the implanted sheets in the SO group; these cells were negative for fast-type myosin heavy chain and desmin (Figure 5, *A–D*). However, a few desmin-positive cells were also detected at the implanted site (Figure 5, *E*). These results suggested that most of the

detected cells had the phenotype of myofibroblasts, whereas a few expressed the phenotype of SMBs. Although these cells might have played an important role in the myocardial regeneration after SMB sheet implantation, their origin and characteristics have not been fully evaluated. Further study will be needed to elucidate the function of these cells and clarify the mechanisms of myocardial regeneration.

mRNA Expressions After Cell-Sheet Implantation

The expression of a variety of molecules that are intramyocardially expressed and potentially related to reverse LV remodeling was assessed by RT-PCR. Among them, the relative expression levels of VEGF and STAT3 mRNA were highest in the SO group, suggesting that the combination of SMB sheets and omentum accelerated the secretion of angiogenesis-related cytokines (ie, VEGF and STAT3) from the SMB sheets in vivo (Figure 6).

Cardiac Functional Recovery

Serial changes in the global systolic and diastolic LV function after cell-sheet implantation were assessed by conventional echocardiography. After the sham operation, LVEDV and LVESV tended to increase until 8 weeks, whereas the LVEF and anterior wall thickness did not change. In contrast, LVEDV did not change in the SO group, but LVESV tended to decrease in the SO and S groups. LVEF increased significantly at 4 and 8 weeks after treatment in the SO group compared with the baseline value. At 4 and 8 weeks after treatment, LVESV was significantly smaller and LVEF significantly greater in the SO group than in the S group, whereas there was no significant difference in LVEDV between them. The anterior wall thickness increased significantly at 8 weeks after treatment in the SO group compared with its baseline value; this change was significantly larger than that in the sham group (Figure 7).

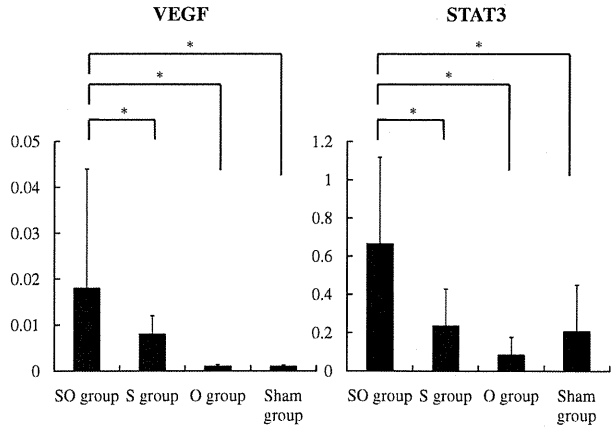

FIGURE 6. mRNA expressions in implanted infarcted hearts were determined by real-time PCR using porcine primers. The expressions of vascular endothelial growth factor *(VEGF)* and signal transducer and activator of transcription 3 *(STAT3)* mRNA were significantly increased in the SO group compared with the other groups. Abbreviations as in Figure 2. N > 4 in each group. *$P < .05$.

DISCUSSION

The major findings of this study were that a new regenerative cell delivery system using SMB sheets covered and wrapped with omentum resulted in the following benefits compared with the conventional method (ie, SMB sheet implantation): (1) a reduced infarct area that led, at least in part, to a thin scar with thick well-vascularized cardiac tissue; (2) angiogenesis induction; and (3) improved cardiac function. Our data suggest that this new cell-delivery system acted in large part by enhancing the paracrine effect of the SMBs.

The mechanism of the restoration of damaged myocardium by SMB sheet implantation is complex, involving many pathways.[5-7] Recent reports describe the beneficial results of SMB sheet implantation in several animal experimental models and patients with heart failure. These benefits were primarily attributed to the secretion of cytokines from the implanted cell sheets (ie, a paracrine effect). It has been suggested that regenerative therapy for the severely damaged myocardium, in which large numbers of cells must be delivered with minimal cell loss, may be achieved by improving the blood perfusion in the region of implanted cells.[7,8] The general intention is to protect the implanted cells from ischemic injury and necrosis by inducing cardiac protective responses (eg, angiogenesis and attenuation of inflammation). A previous study[15] reported that angiogenic factors, such as endothelial cells and some angiogenic growth factors, can enhance angiogenesis to improve the survival of thick-layered cardiomyocyte sheets applied to the damaged myocardium. Shimizu and associates[8] reported that transplanted 3-layered cardiomyocyte sheets could be vascularized in subcutaneous tissue without necrosis, but sheets with 4 or 5 layers had areas with disorganized vasculature and primary ischemia. To overcome this limitation, they performed repeated transplantations of triple-layer grafts, which created a thick myocardium with a well-organized microvascular network.[8] However, technical hurdles still need to be overcome before a similar method can be clinically applied in humans.

In the present study, we demonstrated that the implantation of SMB sheets in combination with omentum was superior to conventional SMB-sheet implantation. The use of an omentum flap to provide revascularization within the ischemic myocardium was previously performed in patients with ischemic heart disease.[9] Although omentopexy alone was not effective for eliciting a rapid recovery, recent basic research studies have suggested a mechanism by which omentum tissue induces angiogenesis.[10,11]

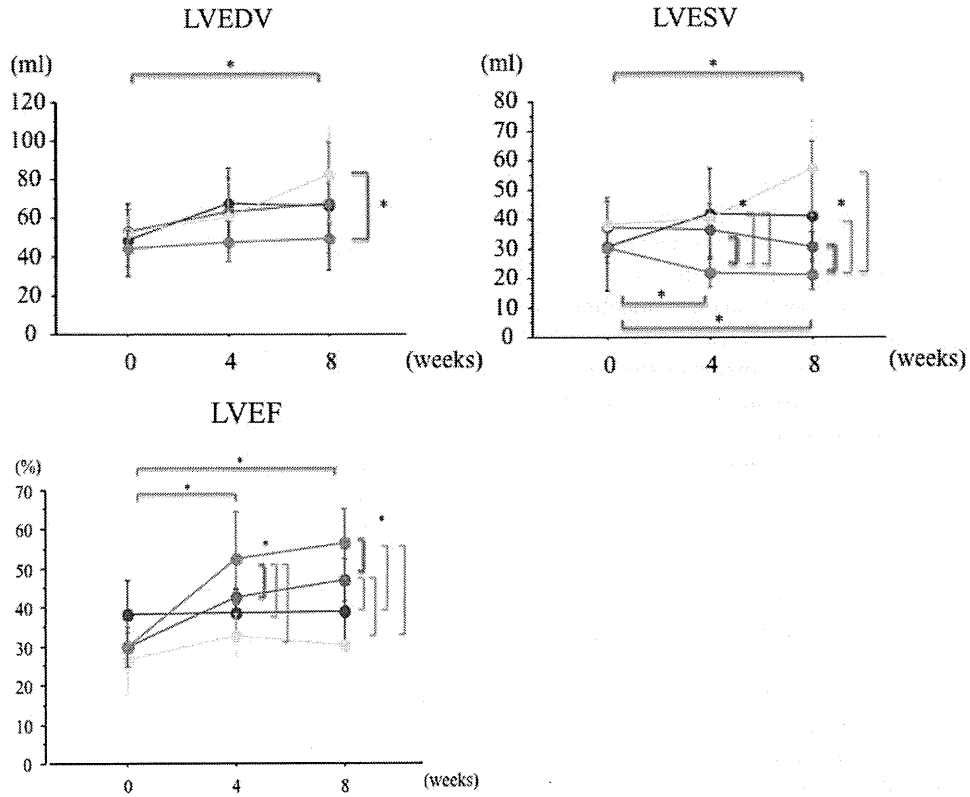

FIGURE 7. Echocardiographic analysis. The SO group showed less ventricular remodeling and greater degrees of improved anterior wall thickness and cardiac function than did the S group. *Pink line,* SO group; *red line,* S group; *blue line,* O group; *green line,* sham group; *LVEDV,* left ventricular end-diastolic volume; *LVESV,* left ventricular end-systolic volume; *LVEF,* left ventricular ejection fraction; other abbreviations as in Figure 2. N = 6 in each group. *$P < .05$.

Omentum flap has often been used by cardiothoracic surgeons to stimulate revascularization. Omentum also has the potential to supply fat-derived stem cells[9] and various cytokines[10,11] and to attenuate inflammation.[12] The adipocytes in omentum release a number of angiogenic growth factors, such as VEGF, suggesting that omentum flap can act as a physiologic exogenous source of multiple angiogenic factors that act synergistically to promote arteriogenesis.[16] Our results support the idea that the interposed omentum enhances the cardiac protection provided by the superimposed SMB sheets, such as by inducing angiogenesis, increasing the blood flow, and prolonging cell survival (in part by attenuating inflammation and protecting the cells from apoptosis). Other experimental studies aimed at enhancing the effects of omentopexy have been reported. Ruel and associates[16] demonstrated that a gastric submucosal patch has excellent angiogenic effects when used as an endogenous source of growth factors in a swine model of chronic myocardial ischemia. Kanamori and colleagues[17] showed that omentopexy enhances the angiogenic effect of cell therapy in a swine model of acute MI. Compared with these studies, our new method seems safer and less invasive because it does not require gastrectomy or bone marrow aspiration.

On the basis of our present results, we speculate that the myocardial functional recovery obtained with the combined method was associated with the upregulation of angiogenic cytokines (eg, VEGF, STAT3) and with increased angiogenesis and blood flow. In addition, the reduced infarct area, as determined by evaluating Masson trichrome–stained hearts, indicates that the animal model used in the present study may be one of hibernating myocardium rather than of chronic infarction.[13] Together with the paracrine effects of the implanted SMB sheet, humoral substances from the omentum might have had beneficial effects on the native cardiomyocytes and viable surrounding muscle cells, preventing global myocardial remodeling. One possible mechanism to explain our results is that the SMB sheet with omentum implantation therapy induced the release of cytokines and enhanced the development of the microvasculature (ie, microcirculation, which is particularly vulnerable to injury during ischemia), which on reperfusion rescued the hibernating myocardium, thereby enhancing the recovery of myocardial performance. A recent report mentioned a possible role of stromal cell–derived factor 1 in recruiting stem cells. Because stromal cell–derived factor 1 is secreted in muscle tissue, and muscle satellite cells express functional CXCR4 receptors, the implanted SMBs may serve

to recruit stem cells to the site of damage, where they promote heart repair.[6] Nevertheless, it remains to be determined what cytokines play a major role in generating therapeutic effects among the many complex molecular and cellular mechanisms involved.

We could find no ventricular premature beat by Holter electrocardiographic analysis after the treatment (data not shown). We[5] previously reported that rat and porcine MI models show less arrhythmia after being treated with SMB-sheet implantation than with needle injection. We speculate that the needle damages the myocardium, which may induce arrhythmia. In contrast, the SMB sheet implantation technique does not normally injure the myocardium. Moreover, we did not observe any cases of lethal ventricular arrhythmia in animals implanted with SMB sheets wrapped with omentum.

CONCLUSIONS

A new cell-delivery method using SMB sheets combined with omentum allowed us to implant large numbers of SMBs in a porcine MI model. The implanted sheets became well-vascularized cardiac tissue, with less scarring and improved cardiac function over that of the animals receiving SMB sheets alone. This method may be applicable for repairing the severely failing heart.

We thank Professor Nariaki Matsuura and Dr Naomasa Kawaguchi of the Department of Pathology, Osaka University Graduate School of Medicine, and Mr Akima Harada for the histologic analysis, Mr Shigeru Matsumi for the excellent technical assistance, Mrs Masako Yokoyama for RT-PCR, and Mrs Yuka Fujiwara and Mr Hiroyuki Shimada for cell culturing. We also thank Dr Leslie Miglietta and Dr Grace Gray for editing our manuscript.

References

1. Menasché P, Hagege AA, Scorsin M, Puzet B, Desnos B, Schwartz K, et al. Myoblast transplantation in heart failure. *Lancet*. 2001;357:279-80.
2. Ghostine S, Carrion C, Souza LC, Richard P, Bruneval P, Vilquin JT, et al. Long-term efficacy of myoblast transplantation on regional structure and function after myocardial infarction. *Circulation*. 2002;106(12 Suppl. 1):I131-6.
3. Hagege AA, Marolleau JP, Vilqiun JT, Alheritiere A, Peyrard S, Duboc D, et al. Skeletal myoblast transplantation in ischemic heart failure: long-term follow-up of the first phase I cohort of patients. *Circulation*. 2006;114(1 Suppl):I108-13.
4. Menasché P, Hagege AA, Vilquin JT, Desnos M, Abergel E, Pouzet B, et al. Autologous skeletal myoblast transplantation for severe postinfarction left ventricular dysfunction. *J Am Coll Cardiol*. 2003;41:1078-83.
5. Miyagawa S, Sawa Y, Sakakida S, Taketani S, Kondoh H, Memon IA, et al. Tissue cardiomyoplasty using bioengineered contractile cardiomyocyte sheets to repair damaged myocardium: their integration with recipient myocardium. *Transplantation*. 2005;80:1586-95.
6. Memon IA, Sawa Y, Fukushima N, Matsumiya G, Miyagawa S, Taketani S, et al. Repair of impaired myocardium by means of implantation of engineered autologous myoblast sheets. *J Thorac Cardiovasc Surg*. 2009;130:646-53.
7. Sekiya N, Matsumiya G, Miyagawa S, Saito A, Shimizu T, Okano T, et al. Layered implantation of myoblast sheets attenuates adverse cardiac remodeling of the infarcted heart. *J Thorac Cardiovasc Surg*. 2009;138:985-93.
8. Shimizu T, Sekine H, Yang J, Isoi Y, Yamato M, Kikuchi A, et al. Polysurgery of cell sheet grafts overcomes diffusion limits to produce thick, vascularized myocardial tissues. *FASEB J*. 2006;20:708-10.
9. O'Shaugnessy L. Surgical treatment of cardiac ischemia. *Lancet*. 1937;232: 185-94.
10. Tabata K, Jiang C, Nemoto S, Saji Y, Ikeda T, Urayama S, et al. A combination of omental flap and growth factor therapy induces arteriogenesis and increased myocardial perfusion in chronic myocardial ischemia: evolving concept of biologic coronary artery bypass grafting. *J Thorac Cardiovasc Surg*. 2006;132:891-9.
11. Shrager JB, Wain JC, Wright CD, Donahue DM, Vlahakes GJ, Moncure AC, et al. Omentum is highly effective in the management of complex cardiothoracic surgical problems. *J Thorac Cardiovasc Surg*. 2003;125:526-32.
12. Levashev YN, Akopov AL, Mosin IV. The possibilities of greater omentum usage in thoracic surgery. *Eur J Cardiothorac Surg*. 1999;15:465-8.
13. Teramoto N, Koshino K, Yokoyama I, Miyagawa S, Ose T, Zeniya T, et al. Experimental pig model of old myocardial infarction with long survival leading to chronic LV dysfunction and remodeling as evaluated by PET. *J Nucl Med*. 2011;52:761-8. Epub 2011 Apr 15.
14. Horiguchi K, Sakakida-Kitagawa S, Sawa Y, Li ZZ, Fukushima N, Shirakura R, et al. Selective chemokine and receptor gene expressions in allografts that develop transplant vasculopathy. *J Heart Lung Transplant*. 2002;21:1090-100.
15. Sekine H, Shimizu T, Hobo K, Sekiya S, Yang J, Yamato M, et al. Endothelial cell coculture within tissue-engineered cardiomyocyte sheets enhances neovascularization and improves cardiac function of ischemic hearts. *Circulation*. 2008; 118(Suppl I):S145-52.
16. Ruel MA, Sellke FW, Bianchi C, Khan TA, Faro R, Zhang JP, et al. Endogenous myocardial angiogenesis and revascularization using a gastric submucosal patch. *Ann Thorac Surg*. 2003;75:1443-9.
17. Kanamori T, Watanabe G, Yasuda T, Nagamine H, Kamiya H, Koshida Y. Hybrid surgical angiogenesis: omentopexy can enhance myocardial angiogenesis induced by cell therapy. *Ann Thorac Surg*. 2006;81:160-8.

Discussion

Dr Vivek Rao *(Toronto, Ontario, Canada).* I have no relevant financial disclosures.

I thank the authors for the courtesy of providing me with a copy of their manuscript well in advance of the meeting. I congratulate them as well for a very elegantly performed and executed study, and I will confirm with the audience that the results shown here are just a small tip of the iceberg of the complete results presented in the manuscript. Most important, the manuscript contains a lot of functional data that, unfortunately, owing to time constraints, Dr Shudo was unable to present.

Having said that, I have a few questions with regard to this study. In the manuscript, it was not quite clear to me whether the number of cell sheets delivered were different between the omentum group (O group) and the cell-sheets-only group (S group). You mentioned that to achieve the omentum wrapping you had a limitation of 5 sheets in the omentum-plus-cell group (SO group). Was that different from the total number of cell sheets implanted in the cell-sheets-only group (S group)?

Dr Shudo. Thank you for your useful comments, Dr Rao.

In this study we used 30 cell sheets total. On the basis of our results in the previous studies, the increase in the number of implanted cell sheets was related to the favorable results, such as enhancing the paracrine effect and improving cardiac function. However, these previous studies also suggested that more than 5 layers of SMB sheets had disorganized vasculature in the implanted site, maybe owing to the primary ischemia. Therefore, in this study, at most 5 layers were attached in one place and covered and wrapped with the omentum to support the angiogenesis.

Dr Rao. I will point to some of the LV function data that were presented in your manuscript. You measured LV function both at 4 weeks and 8 weeks after LAD ligation. What was striking to me was that in most models of LAD ligation there is continued deterioration in LV function in the control groups. In contrast, in your study, the 3 relative control groups had stabilization of their LV

function from 4 to 8 weeks with a continued improvement in LV function in the omentum-plus-cell-transplant group (SO group). Can you explain why the LV function appeared to stabilize in your model.

Dr Shudo. In this study, MI was induced by first ligating the distal portion of the LAD for ischemic preconditioning, followed by placement of the ameroid constrictor around the main trunk of the LAD, just distal to the left circumflex artery branching. It has been reported that the ameroid ring was estimated to occlude inside completely about 2 weeks after being placed in vivo. As you mentioned (and as shown in one slide), LVEF seems to be unchanged 1, 2, and 3 months after placement of the ameroid ring, whereas LVEDV and LVESV indices significantly increased gradually after induction of MI. Therefore, I would like to mention that LV remodeling was successfully obtained in this model in this study.

Dr Rao. I have 1 final question. You showed that the cell retention was approximately double that with the addition of the omentum wrapping, 60% cell retention versus 30% with the cell sheet alone. Yet for almost all of your end points there was absolutely no benefit to cell sheet implantation alone, which is obviously in contrast to many of the studies done previously with SMBs showing a benefit in function, angiogenesis, et cetera. Can you explain why your cell sheet transplant alone had absolutely no benefit in this model.

Dr Shudo. That seems to be a bit confusing. We have obtained good results even in the cell-sheet-only group (S group), too. However, we would like to focus on the preferable results of the new cell-implantation method.

Thank you again for your comments and good questions.

Dr Paul Kurlansky *(Miami, Fla).* I have no disclosures.

This was very interesting work. I have just 2 questions. First, what exact cells or mixture of cells are you putting into the cell sheets? Second, have you looked histologically at the hearts to see if you actually have myocardial regeneration or if you just have hypertrophy and preservation of the residual border zone myocardium?

Dr Shudo. Thank you so much. Regarding the first question, although this is unpublished information, we performed the experimental study about SMBs mixed with adipose tissue, derived mesenchymal stem cells. This model shows priority to the SMB cell-sheet-only group (S group).

Regarding the analysis of border zone, our study using tissue Doppler echocardiography and speckle tracking echocardiography data showed that regional functional recovery was significantly greater in the infarct border region. This result may support the idea that cell-sheet-with-omentum therapy prevented progression of MI by supporting the hibernating myocardium.

Circulation
JOURNAL OF THE AMERICAN HEART ASSOCIATION

American Heart Association®
Learn and Live℠

Induced Adipocyte Cell-Sheet Ameliorates Cardiac Dysfunction in a Mouse Myocardial Infarction Model : A Novel Drug Delivery System for Heart Failure

Yukiko Imanishi, Shigeru Miyagawa, Norikazu Maeda, Satsuki Fukushima, Satoru Kitagawa-Sakakida, Takashi Daimon, Ayumu Hirata, Tatsuya Shimizu, Teruo Okano, Iichiro Shimomura and Yoshiki Sawa

Circulation 2011, 124:S10-S17
doi: 10.1161/CIRCULATIONAHA.110.009993
Circulation is published by the American Heart Association. 7272 Greenville Avenue, Dallas, TX 72514
 Print ISSN: 0009-7322. Online ISSN: 1524-4539

Induced Adipocyte Cell-Sheet Ameliorates Cardiac Dysfunction in a Mouse Myocardial Infarction Model

A Novel Drug Delivery System for Heart Failure

Yukiko Imanishi, PhD; Shigeru Miyagawa, MD, PhD; Norikazu Maeda, MD, PhD; Satsuki Fukushima, MD, PhD; Satoru Kitagawa-Sakakida, MD, PhD; Takashi Daimon, PhD; Ayumu Hirata, MD, PhD; Tatsuya Shimizu, MD, PhD; Teruo Okano, PhD; Iichiro Shimomura, MD, PhD; Yoshiki Sawa, MD, PhD

Background—A drug delivery system that constitutively and effectively retains cardioprotective reagents in the targeted myocardium has long been sought to treat acute myocardial infarction. We hypothesized that a scaffold-free induced adipocyte cell-sheet (iACS), transplanted on the surface of the heart, might intramyocardially secrete multiple cardioprotective factors including adiponectin (APN), consequently attenuating functional deterioration after acute myocardial infarction.

Methods and Results—Induced ACS were generated from adipose tissue–derived cells of wild-type (WT) mice (C57BL/6J), which secreted abundant APN, hepatocyte growth factor, and vascular endothelial growth factor in vitro. Transplanted iACS secreted APN into the myocardium of APN-knockout (KO) mice at 4 weeks. APN was also detected in the plasma of iACS-transplanted APN-KO mice at 3 months (245±113 pg/mL). After left anterior descending artery ligation, iACS, generated from either WT (n=40) or APN-KO (n=40) mice, were grafted onto the surface of the anterior left ventricular wall of WT mice, or only left anterior descending artery ligation was performed (n=43). Two days later, inflammation and infarct size were significantly diminished only in the WT-iACS treated mice. One month later, cardiomyocyte diameter and percent fibrosis were smaller, whereas ejection fraction and survival were greater in the WT-iACS treated mice compared with the KO-iACS–treated or nontreated mice.

Conclusions—Cardioprotective factors including APN, hepatocyte growth factor, and vascular endothelial growth factor were secreted from iACS. Transplantation of iACS onto the acute myocardial infarction heart attenuated infarct size, inflammation, and left ventricular remodeling, mediated by intramyocardially secreted APN in a constitutive manner. This method might be a novel drug delivery system to treat heart disease. (***Circulation.*** **2011;124[suppl 1]:S10–S17.)**

Key Words: acute myocardial infarction ■ adiponectin ■ cell therapy ■ drug delivery system ■ tissue engineering

Despite recent progress in medical and surgical treatments for heart failure, acute myocardial infarction (AMI) and the subsequent deterioration of cardiac performance is still a major cause of death, worldwide. An array of cardioprotective reagents have been identified to be effective in ameliorating AMI by administrating into the infarcted myocardium in experimental models.[1] However, these reagents have failed to show consistent therapeutic efficacy in several clinical trials, probably due to poor retention or rapid inactivation of reagents in the injured myocardial tissues.[1] Therefore, a drug delivery system (DDS) that retains cardioprotective reagents in the targeted myocardial area has long been sought.

Intramyocardially transplanted autologous stem cells secrete various cardioprotective cytokines and growth factors, enhance angiogenesis, reduce fibrosis, attenuate apoptosis, and suppress myocyte hypertrophy, consequently ameliorating AMI in a paracrine manner.[2,3] However, cell transplantation for AMI has shown only modest therapeutic efficacy in large-scale clinical studies. It appears to result from insufficient paracrine effects whose magnitude and figure are largely affected by the cell delivery method or transplanted cell source.[4] To enhance the survival and functions of the transplanted cells, we developed a cell-sheet–based delivery method in which isolated cells, cultivated in vitro as a sheet without a scaffold, are simply placed on the surface of the myocardium. This treatment enhances the paracrine effects, resulting in better therapeutic efficacy.[5,6]

Adipocytes differentiated from adipose tissue–derived stromal-vascular fraction (SVF) cells are a promising cell

From the Department of Cardiovascular Surgery (Y.I., S.M., S.F., S.K.-S., Y.S.) and the Department of Metabolic Medicine (N.M., A.H., I.S.), Graduate School of Medicine, Osaka University, Suita, Osaka, Japan; the Division of Biostatistics (T.D.), Department of Mathematics, Hyogo College of Medicine, Nishinomiya, Hyogo, Japan; and the Institute of Advanced Biomedical Engineering and Science (T.S., T.O.), Tokyo Women's Medical University, Shinjuku-ku, Tokyo, Japan.

Presented at the 2010 American Heart Association meeting in Chicago, IL, November 12–16, 2010.

The online-only Data Supplement is available at http://circ.ahajournals.org/lookup/suppl/doi:10.1161/CIRCULATIONAHA.110.009993/-/DC1.

Correspondence to Yoshiki Sawa, 2-2 Yamada-oka, Suita City, Osaka 565-0871, Japan. E-mail sawa@surg1.med.osaka-u.ac.jp

Circulation **is available at http://circ.ahajournals.org** **DOI: 10.1161/CIRCULATIONAHA.110.009993**

source for treating AMI because as they secrete hepatocyte growth factor (HGF), vascular endothelial growth factor (VEGF), and, importantly, adiponectin (APN).[7,8] APN is a circulating secretory protein that has multiple cardioprotective effects, including the attenuation of inflammation, fibrosis, and myocyte hypertrophy.[8,9] However, the clinical use of APN for treating AMI has been hampered by the lack of effective systems for delivering APN to the heart. We hypothesized that using cell-sheet technology to deliver adipocytes that secrete multiple cardioprotective factors, including APN, might attenuate the functional deterioration after AMI.

Methods

Animal care complied with the "Guide for the Care and Use of Laboratory Animals" (NIH publication No. 85 to 23, revised 1996). Experimental protocols were approved by the Ethics Review Committee for Animal Experimentation of Osaka University Graduate School of Medicine.

Generation and Assessment of Adipocyte Cell-Sheet

The SVF cells of adipose tissue were isolated from wild-type (WT; male C57BL/6J) or APN-knockout (KO) mice,[10] as described previously.[11] The isolated SVF cells were cultured until they become confluent on Upcell dishes (CellSeed Inc, Tokyo, Japan). Differentiation into adipocytes was induced by insulin, dexamethasone, isobutylmethylxanthine, and pioglitazone (Sigma-Aldrich, MO). Incubation at 20°C induced the cells to detach from the culture dishes, yielding a scaffold-free cell-sheet, which we call an "induced adipocyte cell-sheet" (iACS). The secretion of HGF, VEGF, leptin, interleukin (IL)-6, tumor necrosis factor (TNF)-α, and IL-10 into the culture supernatant was assessed by ELISA. Before transplantation, WT mouse–derived iACS (WT-iACS) and APN-KO mouse–derived iACS (KO-iACS) were labeled with the use of a PKH26 kit (Sigma-Aldrich).

Generation of AMI Model and Cell-Sheet Transplantation

An AMI model was generated by permanent ligation of the left anterior descending artery (LAD) in male C57BL/6J mice, 10 to 15 weeks old.[12] The mice were anesthetized by isoflurane inhalation (Mylan Inc). Five minutes after the LAD ligation, WT-iACS (W group, n=40) or KO-iACS (K group, n=40) was grafted onto the surface of the anterior left ventricular (LV) wall, or a sham operation was performed (C group, n=43). The mice were euthanized at 2 and 28 days after LAD ligation and cell-sheet transplantation.

Assessment of Cardiac Function and Survival

Cardiac function was assessed with the use of an echocardiography system equipped with a 12-MHz transducer (GE Healthcare) at 4 weeks. The LV dimensions were measured, and LV ejection fraction was calculated as $(LVDd^3-LVDs^3)/LVDd^3\times100$, where LVDd and LVDs are the LV end-diastolic and end-systolic dimensions, respectively.[12] The mice were housed in a temperature-controlled incubator for 50 days after treatment to determine their survival.

Histological Analysis

Freshly excised hearts were stained with 1% 2,3,5-triphenyltetrazolium chloride (TTC; Sigma-Aldrich). The red-stained infarct area was quantified by computerized planimetry, using MetaMorph Software (Molecular Devices). Frozen sections (8 μm) of hearts and cell-sheets were stained with antibodies against APN (Otsuka Pharmaceutical, Tokushima, Japan) or CD11b (Abcam, Cambridge, UK). The secondary antibody was Alexa 488 goat anti-rabbit (Life Technologies). Counterstaining was performed with 6-diamidino-2-phenylindole (Life Technologies). To analyze the myocardial collagen accumulation, heart sections were stained with Masson trichrome. The collagen volume fraction was calculated in the peri-infarct area. To assess cardiomyocyte diameter, heart sections were stained with periodic acid-Schiff. MetaMorph Software was used for the quantitative morphometric analysis.

Cytokine Antibody Array

Proteins were isolated from whole-heart samples and analyzed using a Milliplex Mouse Cytokine/Chemokine Panel Premixed 32Plex, according to the manufacturer's instructions (Millipore).

Quantitative Real-Time PCR

Total RNA was isolated from the peri-infarct area by use of the RNeasy Mini Kit and reverse-transcribed, using Omniscript Reverse transcriptase (Qiagen, Hilden, Germany). Quantitative PCR was performed with the PCR System (Life Technologies). The expression of each mRNA was normalized to that of glyceraldehyde-3-phosphate dehydrogenase.

Statistical Analysis

Data are expressed as the mean±SEM. The data distributions were checked for normality with the Shapiro-Wilk test and for equality of variances with the Bartlett test. Comparisons between 2 groups were made using the unpaired t test or the Wilcoxon-Mann-Whitney U test, as appropriate. For comparisons among 3 groups, we used 1-way ANOVA, followed by Fisher protected least-significance difference test or the Kruskal-Wallis test, followed by the post hoc pairwise Wilcoxon-Mann-Whitney U test, as appropriate. The survival curves were prepared by using the Kaplan-Meier method and were compared using the overall log-rank test, followed by the post hoc pairwise log-rank test. The multiplicity in pairwise comparisons was corrected by the Benjamin-Hochberg procedure. All probability values are 2-sided, and values of $P<0.05$ were considered to indicate statistical significance. Statistical analysis was performed with the StatView 5.0 Program (Abacus Concepts, Berkeley, CA) and the R program.[13]

An expanded Methods section can be found in the online-only Data Supplement.

Results

Characterization of the Adipocyte Cell-Sheets

Most SVF cells differentiated into mature adipocytes bearing oil droplets by 7 days after differentiation induction. Induced ACS or undifferentiated SVF cell-sheets were then generated by lowering the temperature (Figure 1A). Each iACS was approximately 7 mm in diameter (Figure 1B) and 100 μm thick (Figure 1C). WT-iACS expressed abundant APN in the cytoplasm and extracellular matrix around the oil-droplet–rich adipocytes, as assessed by immunohistochemistry (Figure 1D) and ELISA (Figure 1E). In contrast, neither the SVF cell-sheets of either origin nor the KO-iACS expressed APN (Figure 1D and 1E). The ELISA showed abundant HGF expression in WT-iACS and KO-iACS, which was down-regulated compared with the WT SVF cells (Figure 1F). The secretion of VEGF and leptin was remarkably enhanced by the SVF cell differentiation into adipocytes. IL-6 and IL-10 were secreted by the WT-iACS and WT-SVF cells at similar levels, which were lower than the levels secreted by KO-iACS. The secretion of TNF-α was not evident in any group because the cell-free culture medium also contained 2.29 pg/mL TNF-α.

Transplanted Induced ACS Supplied APN to the Myocardium

WT-iACS were transplanted onto the heart of intact APN-KO mice to evaluate behavior of the WT-iACS, including APN

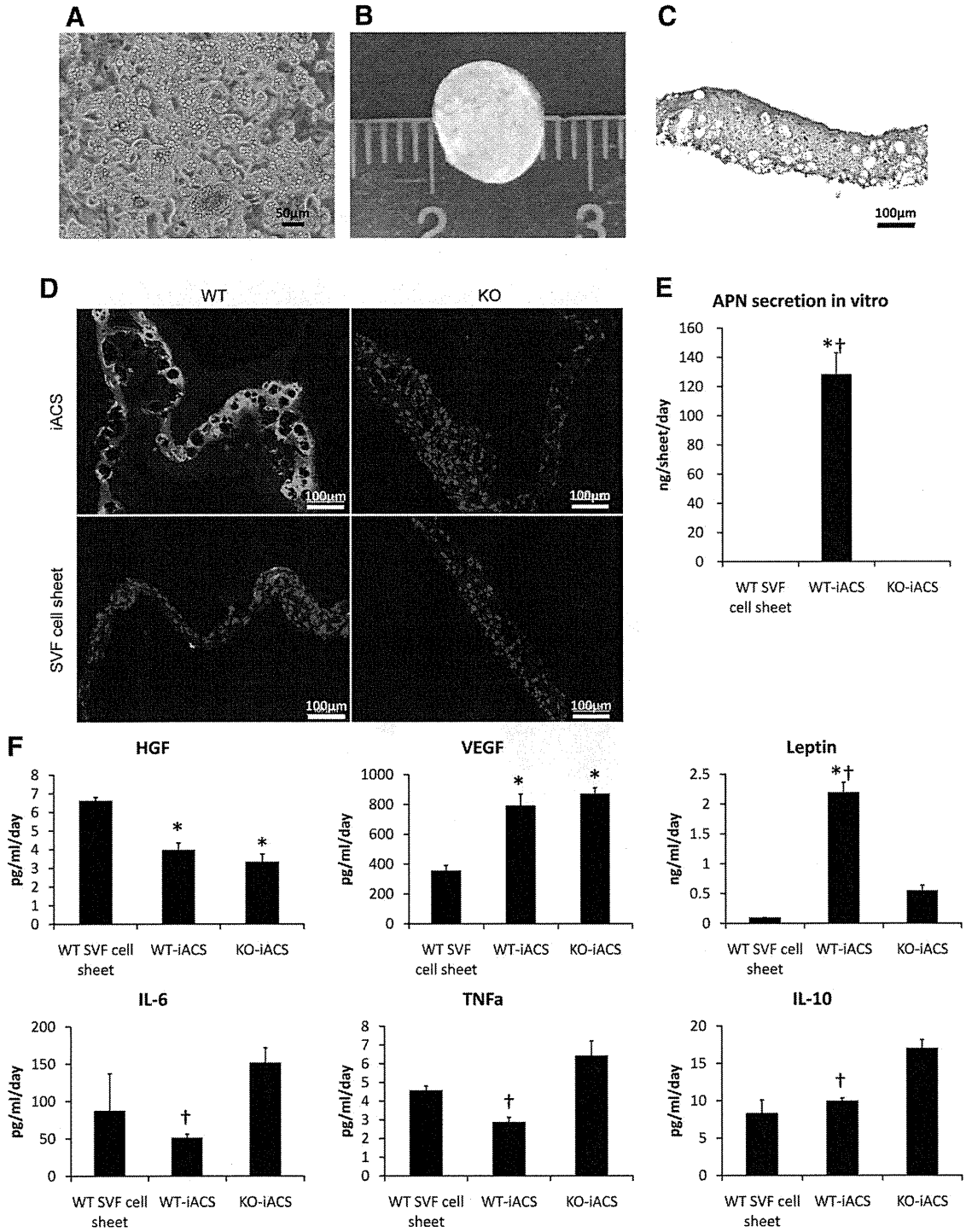

Figure 1. Characterization of induced adipocyte cell-sheet (iACS) in vitro. **A**, Histological analysis showing mature adipocytes with oil droplets in the cytosol. **B**, Induced ACS detached from the temperature-responsive culture dish. **C**, Cross-sectional view of hematoxylin and eosin–stained iACS. **D**, Representative pictures of adiponectin (APN)-stained cell-sheets. Wild-type (WT)-iACS showed strong labeling for APN. The WT stromal-vascular fraction (SVF) cell-sheet, knockout (KO)-iACS, and KO SVF cell-sheet were negative for APN. Green indicates APN; blue, nuclei. **E**, APN secretion into the WT-iACS culture supernatant determined by ELISA (WT SVF cell sheet, n=2; WT-iACS, n=5; KO-iACS, n=8; $P<0.05$, Kruskal-Wallis test). *$P<0.05$ versus WT SVF cell-sheet, †$P<0.05$ versus KO-iACS, post hoc Wilcoxon-Mann-Whitney *U* test. **F**, Hepatocyte growth factor (HGF), vascular endothelial growth factor (VEGF), leptin, interleukin (IL)-6, IL-10, and tumor necrosis factor (TNF)-α secretion into the culture supernatant, measured by ELISA. WT-iACS secreted HGF, VEGF, leptin, IL-6, and IL-10 but not TNF-α (WT SVF cell sheet, n=2; WT-iACS, n=8 to 12; KO-iACS, n=6 to 9). HGF, VEGF, and leptin ($P<0.05$, ANOVA); *$P<0.05$ versus WT SVF cell-sheet, †$P<0.05$ versus KO-iACS, post hoc Fisher protected least-significance difference test. TNF-α, IL-6, and IL-10 ($P<0.05$, Kruskal-Wallis test); *$P<0.05$ versus WT SVF cell-sheet, †$P<0.05$ versus KO-iACS, post hoc Wilcoxon-Mann-Whitney *U* test.

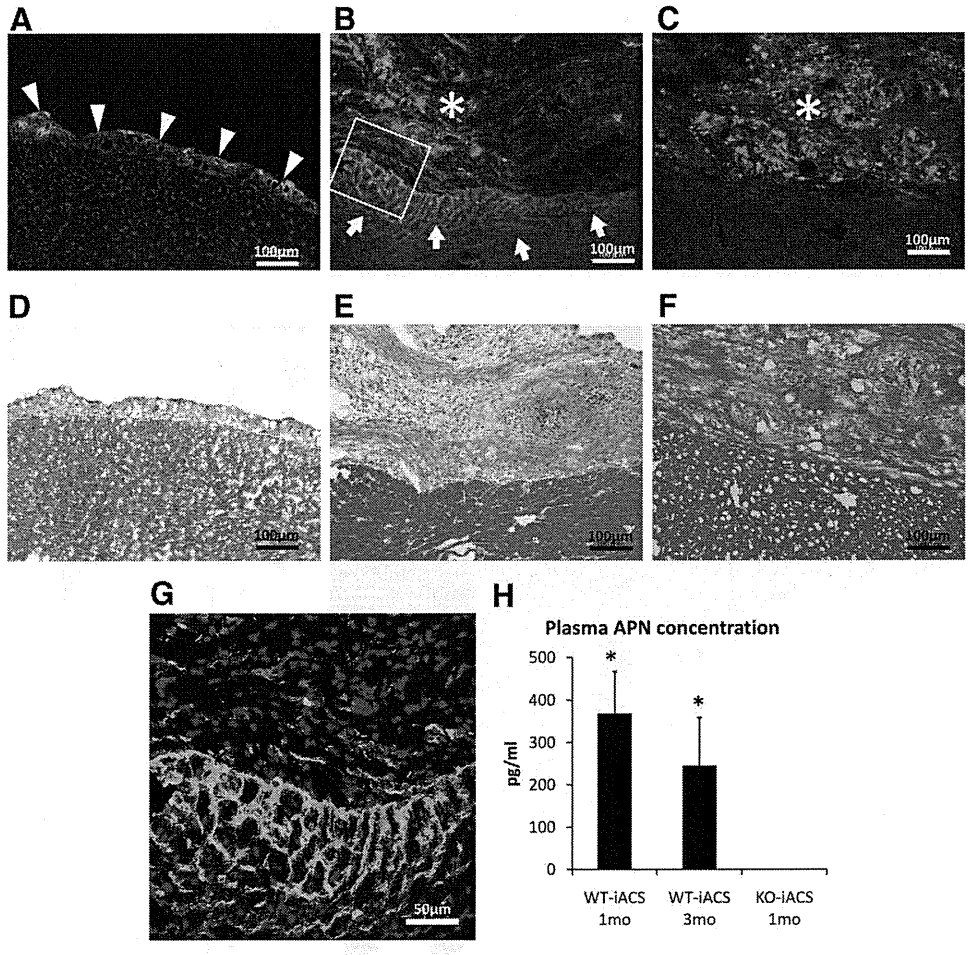

Figure 2. Local and systemic delivery of induced adipocyte cell-sheet (iACS)-derived adiponectin (APN) in vivo. **A**, Immediately after wild-type (WT)-iACS implantation onto the knockout (KO) mouse heart, iACS-expressed APN was detected on the epicardium. Arrowheads show the implanted WT-iACS. Green indicates APN; blue, nuclei. **B**, WT-iACS stained with red fluorescent dye were implanted onto KO myocardium. Twenty-eight days after transplantation, APN was detected both in the surviving WT-iACS and the extracellular matrix (ECM) of the KO mouse myocardium at the implanted site. Asterisk indicates the implanted WT-iACS. Arrows show iACS-derived APN in the host myocardium. **C**, KO-iACS stained with red fluorescent dye and implanted onto KO myocardium. Twenty-eight days after transplantation, the implanted KO-iACS survived, but no APN was detected in the KO-iACS or the ECM. Asterisk indicates the implanted KO-iACS. Green indicates APN; red, KO-iACS; and blue, nuclei. **D** through **F**, Hematoxylin and eosin staining of a serial section from the sample in **A**, **B**, and **C**, respectively. **G**, High-magnification image of the square in **B** and **H**. Plasma APN concentration of WT-iACS (WT) or KO-iACS (KO) recipient APN-KO mice. APN was detected in the WT group plasma 1 (n=4) and 3 months (n=3) after transplantation but not in the KO group plasma (n=4, $P<0.05$, Kruskal-Wallis test). *$P<0.05$ versus KO 1 month, post hoc Wilcoxon-Mann-Whitney *U* test.

production. Immediately after transplantation, the WT-iACS expressed APN epicardially at the anterior LV wall, but it was not expressed intramyocardially (Figure 2A). Four weeks after transplantation, the WT-iACS had survived, was approximately 600 μm thick, and contained adipocytes and connective tissue. At this time, the WT-iACS was tightly integrated with the epicardium, but no invasion of transplanted cells into the recipient myocardium was observed (Figure 2B and 2E). APN was expressed in the cytoplasm of scattered surviving WT-iACS cells and in the myocardium close to the WT-iACS (Figure 2B and 2G). In contrast, although the KO-iACS transplanted into KO mice survived (Figure 2C and 2F), they did not express or secrete APN (Figure 2C). When WT-iACS was transplanted into KO mice, APN was detected in the plasma 1 and 3 months later, but it was not detected in the plasma of KO mice with the KO-iACS implant (Figure 2H).

Induced ACS Implantation Reduced Inflammatory Responses and Infarct Area 2 Days After MI

The anti-inflammatory effects of WT-iACS were evaluated by cytokine antibody array analysis of whole-heart lysates from the AMI mice that were treated with WT-iACS (W), KO-iACS (K), or no iACS (C) groups at 2 days after implantation (Table). A significantly lower level of the inflammatory factor granulocyte macrophage colony-stimulating factor (GM-CSF) was observed in the W group compared with the others, and the levels of other inflammatory cytokines, keratinocyte chemoattractant, IL-6, granulocyte (G)-CSF, and monocyte chemotactic protein-1 (MCP-1) showed a trend toward downregulation in the W group. Quantitative RT-PCR showed that the TNFα mRNA levels were lower in the peri-infarct area of the W group than in that of the K and C groups, which reached statistical significance in the W group (Figure 3A). Furthermore, immunohistochem-

Table. Cytokine Antibody Array

	W Group (n=4)	K Group (n=5)	C Group (n=6)
Granulocyte macrophage colony-stimulating factor, pg	0.0±0*†	21.8±1.3	18.5±6.7
Keratinocyte chemoattractant, pg	292.7±42.7	539.9±56.4	629.9±113.1
Interleukin-6, pg	175.3±16.0	295.3±44.0	281.4±51.5
Granulocyte-colony stimulating factor, pg	37.6±5.7	94.6±35.0	52.8±9.5
Monocyte chemotactic protein-1, pg	316.4±51.9	467.6±50.4	388.7±87.1

$P<0.05$, Kruskal-Wallis test.
*$P<0.05$ versus C group.
†$P<0.05$ versus K group, post hoc Wilcoxon-Mann-Whitney U test.

istry for CD11b showed significantly fewer infiltrated macrophages in the peri-infarct area of the W and K groups than in that of the C group (Figure 3B). Finally, a semiquantitative assessment by TTC staining showed that the infarct area was significantly smaller in the W group than in the K and C groups (Figure 4).

Induced ACS Transplantation Suppressed LV Remodeling Development at 4 Weeks After MI

Four weeks after LAD ligation, the C group showed a typical MI with a large anterior LV scar, dilatation of the LV cavity, and cardiomyocyte hypertrophy. By comparison, the LV of the W group was less dilated, and the anterior wall was thicker (Figure 5A). The diameter of the cardiomyocytes was significantly smaller in the W group (Figure 5B and 5C), and there was less collagen accumulation (Figure 5D and 5E). There was no difference in capillary density among the groups (online-only Data Supplement Figure 1).

Therapeutic Effects of Induced ACS Transplantation on Cardiac Performance and Survival at 4 Weeks After MI

Cardiac performance was evaluated by 2D echocardiography 4 weeks after implantation. Both the diastolic and systolic LV dimensions were smaller in the W group than the others, but the difference was not significant. In contrast, LV ejection fraction was significantly greater in the W group than the K and C groups (Figure 6A). In addition, in a WT-iACS–transplanted rat model of acute MI, invasive hemodynamic analysis showed higher end-systolic pulmonary vascular resistance and dP/dtmax and lower dP/dtmin, compared with sham transplantation (online-only Data Supplement Figure 2). Mortality was substantial until 14 days after LAD ligation in the K and C groups. In contrast, in the W group, there was little mortality 5 days after MI and thus a significant difference in survival (Figure 6B).

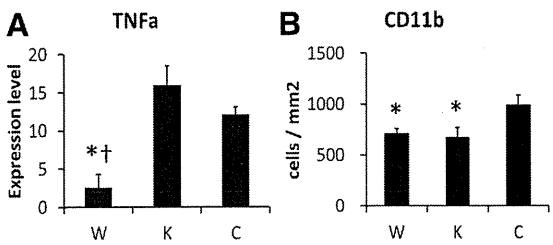

Figure 3. Induced adipocyte cell-sheet (iACS) effects on inflammatory responses after myocardial infarction at the implant/myocardium border zone 2 days after implantation. **A**, Quantitative RT-PCR results for the tumor necrosis factor (TNF)-α transcript. TNF-α transcription was significantly lower in the W group (n=4) than in the K (n=4) and C groups (n=6, $P<0.05$, Kruskal-Wallis test) *$P<0.05$ versus C group, †$P<0.05$ versus K group, post hoc Wilcoxon-Mann-Whitney U test. **B**, Quantification of CD11b-positive cells. The number of CD11b-positive cells was significantly lower in the W (n=4) and K (n=4) groups than in the C group (n=6, $P<0.05$, ANOVA). *$P<0.05$ versus C group, Fisher protected least-significance difference test.

Discussion

We developed an adipocyte cell-sheet–based DDS for the heart. These sheets, which are generated from adipose tissue–derived SVF cells induced to differentiate in culture, secreted multiple cardioprotective factors in vitro, including APN, HGF, and VEGF. Although adipose tissue–derived SVF cells had no ability to secrete APN, after the differentiation to adipocytes, the cells started to secrete APN in addition to HGF and VEGF. APN was secreted from the iACS into the myocardium and blood for at least 3 months, probably along with HGF, VEGF, leptin, and IL-10. In a mouse model of AMI, WT-iACS significantly decreased inflammation and myocardial infarct size at the acute stage. Furthermore, myocardial fibrosis and cardiomyocyte hypertrophy were significantly attenuated at the late stage, which led to improved cardiac performance and a better post-MI survival rate. Importantly, the transplantation of KO-iACS onto infarcted hearts resulted in only modest therapeutic benefits, indicating that APN plays a pivotal role in attenuating the AMI in this experimental model.

There have been many experimental and clinical studies in which the administration of exogenous proteins, including APN, induced angiogenesis, reversed remodeling, and improved cardiac function.[1,14] The issues in this method may be that naked protein is delivered to the heart and is often poorly retained or quickly inactivated and therefore lacks long-term efficacy.[15] MI is a progressive disease, characterized by massive ischemic necrosis of the myocardial tissue and subsequent inflammation. This leads to cardiac remodeling that exacerbates the oxygen shortage in the surviving cardiac tissue. These pathological and functional deteriorations eventually cause end-stage heart failure. A constitutive and balanced supply of cardioprotective reagents, rather than the 1-time administration of a single reagent, should inhibit this vicious circle. The direct injection of plasmid vectors encoding targeted reagents and the transplantation of genetically modified cells can provide a controlled and stable supply of reagents over the long term; however, their clinical use is limited because the safety of the viral systems used as vectors for the plasmids and of modifying cells for transplant is still a concern.[16] Encapsulation as the DDS for biomaterials is another attractive approach; however, difficulty in controlling the rate of reagent release, such as the occurrence of an initial burst release, limits its therapeutic efficacy.[17,18] In addition, biodegradable polymers that carry reagents may induce the deposition of extracellular matrix and myocardial inflamma-

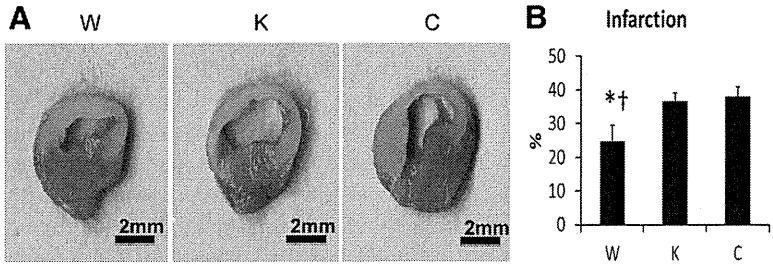

Figure 4. Infarct area of induced adipocyte cell-sheet (iACS)-treated heart 2 days after myocardial infarction. **A**, Representative 2,3,5-triphenyltetrazolium chloride staining images at border zone of infarct. **B**, Quantification of infarct size. The percent infarcted area was significantly lower in the W group (n=8) compared with the other groups (K, n=7; C, n=9; $P<0.05$, ANOVA). *$P<0.05$ versus C group. †$P<0.05$ versus K group, Fisher protected least-significance difference test.

tion, leading to pathological fibrotic states.[19] Our cell-sheet–based DDS constitutively and effectively delivered multiple cardioprotective factors over the long term, leading to reverse LV remodeling after MI, without gene modification or scaffold use. Thus, this strategy might be more practical and effective than other methods for delivering therapeutic proteins for treating MI in the clinical arena.

It is possible that the delivery of multiple growth factors will improve therapeutic efficacy over the delivery of a single factor. This hypothesis is supported by a study showing that the combination of HGF and VEGF leads to better engraftment and significant angiogenesis, compared with either factor alone.[20] In our study, the KO-iACS, which secreted HGF and VEGF but not APN, reduced macrophage infiltration but did not induce functional or survival benefits. These benefits were conferred by the WT-iACS, which produced APN, suggesting that APN's benefits are different from and in addition to those of known paracrine mediators, such as HGF or VEGF.

APN is a protective factor against cardiovascular diseases.[9,21] In particular, its anti-inflammatory properties may be the major reason for its beneficial effects on cardiovascular disorders, because APN-deficient mice exhibit increased TNF-α production and myocardial apoptosis in response to ischemia reperfusion.[22,23] We observed that the expression of TNF-α in the AMI heart was significantly reduced by transplanting WT-iACS but not KO-iACS, which secrete similar levels of the same cytokines, except for APN, suggesting that the direct anti-inflammatory effects of APN played a key role in the attenuated inflammation in this study. In addition, the infarct size was significantly smaller in the WT-iACS–transplanted hearts than in the KO-iACS–transplanted ones. Infarct size is determined by multiple factors, including the magnitude of ischemic stimuli, degree of

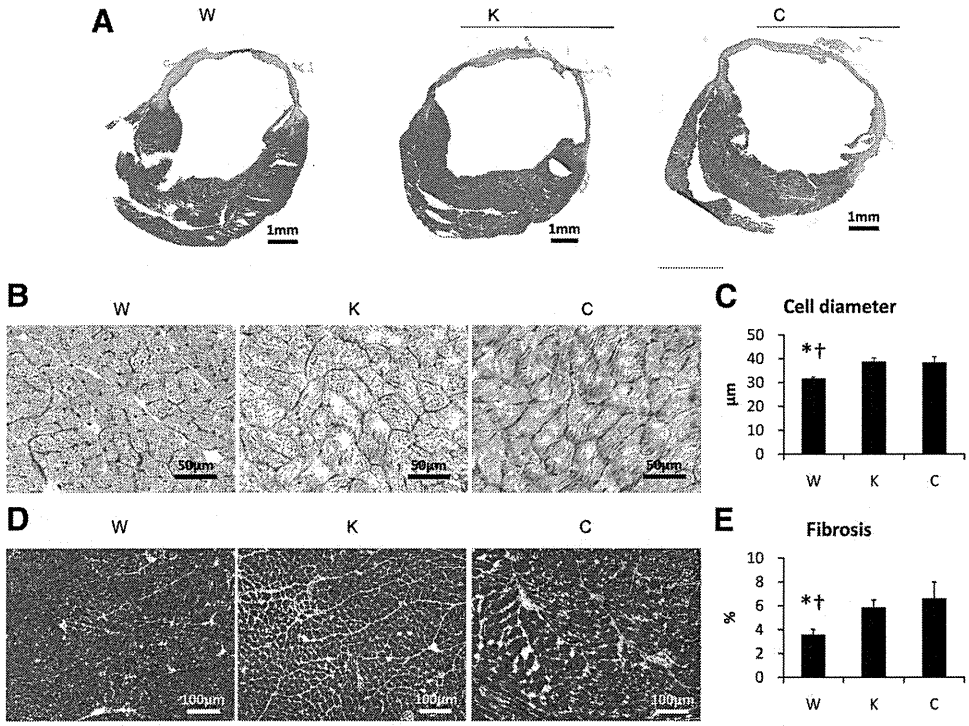

Figure 5. Effects on left ventricular remodeling by induced adipocyte cell-sheet (iACS) transplantation 4 weeks after myocardial infarction. **A**, Representative macro images from each group. **B**, Representative periodic acid-Schiff staining of tissue remote from infarct site. **C**, Quantification of cardiomyocyte diameter. Cardiomyocyte diameters in the tissue remote from the infarct site were significantly smaller in the W group (n=6) than in the other groups (K, n=8; C, n=5; $P<0.05$, ANOVA). *$P<0.05$ versus C group. †$P<0.05$ versus K group, Fisher protected least-significance difference test. **D**, Representative Masson trichrome staining images at the border area. **E**, Quantification of percent fibrosis. Fibrosis at the border area was significantly suppressed in the W group (n=6) compared with the other groups (K, n=8; C, n=5; $P<0.05$, Kruskal-Wallis test). *$P<0.05$ versus C group. †$P<0.05$ versus K group, post hoc Wilcoxon-Mann-Whitney *U* test.

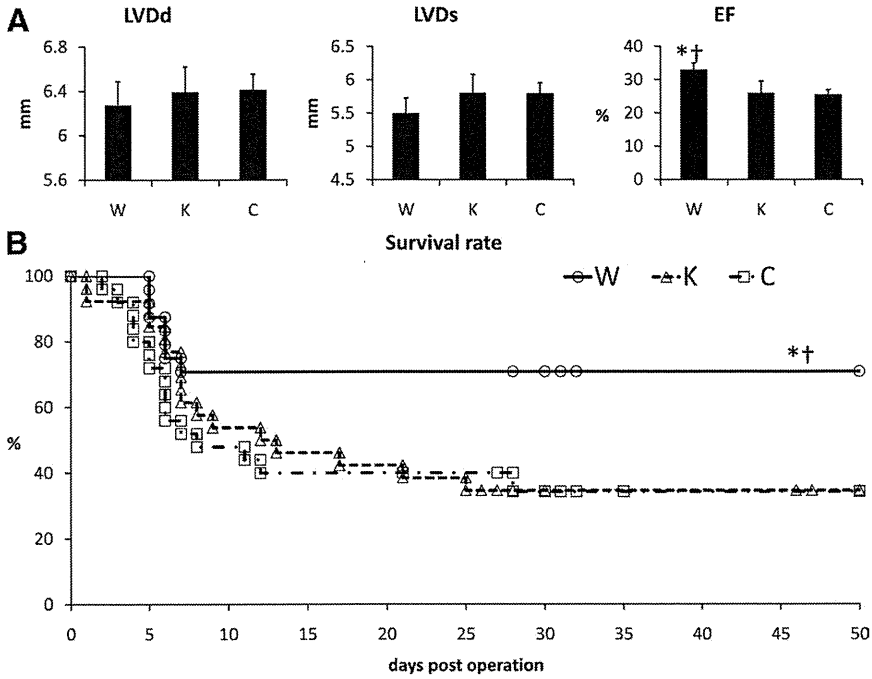

Figure 6. Wild-type induced adipocyte cell-sheet (WT-iACS) improved cardiac function and survival after myocardial infarction. **A**, Evaluation of cardiac performance 4 weeks after treatment (n=18 each). In the W group, the left ventricular end-systolic dimension was smaller and the ejection fraction significantly higher than in the other groups ($P<0.05$, Kruskal-Wallis test). *$P<0.05$ versus C group. †$P<0.05$ versus K group, post hoc Wilcoxon-Mann-Whitney *U* test. **B**, Survival rates after treatment. There was no significant difference between the C (n=25) and K groups (n=26). The W group (n=24) showed significantly better survival than the other groups ($P<0.05$, overall log-rank test). *$P<0.05$ versus C group, †$P<0.05$ versus K group, post hoc log-rank test.

inflammation, and amount of apoptosis. The beneficial effects of APN on inflammation after the iACS treatment may have led to the attenuated infarct size and suppressed the exacerbation of cardiac performance. In addition, APN has been shown to directly inhibit the hypertrophic response in myocytes.[24] Therefore, the combined direct and indirect actions of APN probably inhibit the development of pathological hypertrophy and preserve myocardial mass. Although we traced the iACS-derived APN by using APN-KO mice to demonstrate the APN delivery, HGF, VEGF, and other beneficial growth factors are probably also released constitutively by the iACS. Thus, iACS can provide a combined and balanced release of multiple paracrine mediators that may synergistically augment therapeutic benefits.[20,23]

On the other hand, APN is reported to have proangiogenic potential.[9] In fact, VEGF secretion from WT-iACS and KO-iACS were also greater compared with undifferentiated WT-SVF cell-sheet in this study. However, the capillary density in the treated myocardium, which was assessed by CD31 immunohistolabeling, was not higher at 28 days after WT-iACS transplantation, compared with post–KO-iACS transplantation and sham transplantation. These inconsistent findings may result from the AMI model in which neoangiogenesis substantially occurs in the treated area, not allowing dissection of the slight difference in capillary density between the experimental groups. Rather, the findings of this study suggested that anti-inflammatory effects were the major mechanism for the improvement after WT-iACS transplantation in this model. Another disease model such as dilated cardiomyopathy and old myocardial infarction may be more appropriate to evaluate angiogenic property of iACS treatment.

The treatment strategy for AMI studied here is not directly applicable to the clinical arena, because the time required to isolate, cultivate, or manipulate cells in vitro is not available for AMI, which requires immediate treatment. However, the finding that this therapy yielded marked cardioprotective effects through constitutive APN production should be beneficial for treating other types of cardiac pathologies, such as the chronic phase of MI, dilated cardiomyopathy, or myocarditis. In addition, this sophisticated cell-sheet, which elevates the systemic APN level for some time, might also be effective for treating systemic disorders such as obesity-linked cardiovascular or metabolic disorders, although this possibility will require further investigation.[9,21]

A potential limitation of this study is that the small sample sizes in our experiments limit their statistical power. Thus, the apparent absence of a statistical difference may be due to the lack of statistical power to detect small differences; therefore our negative results may have no meaning. Nevertheless, despite the small sample sizes, we at least clearly showed that APN was delivered by WT-iACS and that the therapeutic effect of WT-iACS implantation was attained through APN. Furthermore, we conducted multiple statistical tests for significance separately for each outcome in a univariate manner, although we adjusted for multiple pairwise testing between groups within each outcome. Such tests for multiple outcomes could lead to the inflation of the type I error probability in making treatment effect claims.

In the present study, we focused on the delivery of cytokines by iACS. However, we speculate that other mechanisms may also contribute to the functional recovery after iACS implantation. Tateno et al[25] clearly showed that cell transplantation induces the recipient tissue to produce angiogenic factors, including IL-1β, even though the transplanted cells do not produce sufficient levels of cytokines to promote angiogenesis directly. Similarly, iACS may stimulate recipient tissue, thus activating cells in the recipient to produce angiogenic cytokines. Further study will be required to elucidate what cross-talk occurs between the iACS and the recipient myocardium.

In summary, iACS may be a powerful DDS for cytokines, including APN, HGF, and VEGF. The implantation of iACS onto the infarcted mouse heart reduces the infarct size, inflammation, and LV remodeling. This method is probably adaptable as a novel DDS for treating heart failure.

Acknowledgments

We thank Masako Yokoyama and Yoko Motomura for excellent technical assistance.

Sources of Funding

This study was funded in part by a grant-in-aid for Scientific Research (22659251) from the Ministry of Education, Culture, Sports, Science, and Technology of Japan.

Disclosures

Dr Shimizu is a consultant for CellSeed, Inc. Dr Okano is an Advisory Board Member in CellSeed, Inc, and an inventor/developer designated on the patent for temperature-responsive culture surfaces.

References

1. Hwang H, Kloner RA. Improving regenerating potential of the heart after myocardial infarction: factor-based approach. *Life Sci.* 2010;86:461–472.
2. Vandervelde S, van Luyn MJ, Tio RA, Harmsen MC. Signaling factors in stem cell-mediated repair of infarcted myocardium. *J Mol Cell Cardiol.* 2005;39:363–376.
3. Gnecchi M, Zhang Z, Ni A, Dzau VJ. Paracrine mechanisms in adult stem cell signaling and therapy. *Circ Res.* 2008;103:1204–1219.
4. Herrmann JL, Abarbanell AM, Weil BR, Wang Y, Wang M, Tan J, Meldrum DR. Cell-based therapy for ischemic heart disease: a clinical update. *Ann Thorac Surg.* 2009;88:1714–1722.
5. Miyagawa S, Saito A, Sakaguchi T, Yoshikawa Y, Yamauchi T, Imanishi Y, Kawaguchi N, Teramoto N, Matsuura N, Iida H, Shimizu T, Okano T, Sawa Y. Impaired myocardium regeneration with skeletal cell sheets–a preclinical trial for tissue-engineered regeneration therapy. *Transplantation.* 2010;90: 364–372.
6. Shimizu T, Sekine H, Yamato M, Okano T. Cell sheet-based myocardial tissue engineering: new hope for damaged heart rescue. *Curr Pharm Design.* 2009;15:2807–2814.
7. Nakagami H, Morishita R, Maeda K, Kikuchi Y, Ogihara T, Kaneda Y. Adipose tissue-derived stromal cells as a novel option for regenerative cell therapy. *J Atheroscler Thromb.* 2006;13:77–81.
8. Maeda K, Okubo K, Shimomura I, Funahashi T, Matsuzawa Y, Matsubara K. CDNA cloning and expression of a novel adipose specific collagen-like factor, apm1 (adipose most abundant gene transcript 1). *Biochem Biophys Res Commun.* 1996;221:286–289.
9. Shibata R, Ouchi N, Murohara T. Adiponectin and cardiovascular disease. *Circ J.* 2009;73:608–614.
10. Maeda N, Shimomura I, Kishida K, Nishizawa H, Matsuda M, Nagaretani H, Furuyama N, Kondo H, Takahashi M, Arita Y, Komuro R, Ouchi N, Kihara S, Tochino Y, Okutomi K, Horie M, Takeda S, Aoyama T, Funahashi T, Matsuzawa Y. Diet-induced insulin resistance in mice lacking adiponectin/acrp30. *Nat Med.* 2002;8:731–737.
11. Planat-Benard V, Silvestre JS, Cousin B, Andre M, Nibbelink M, Tamarat R, Clergue M, Manneville C, Saillan-Barreau C, Duriez M, Tedgui A, Levy B, Penicaud L, Casteilla L. Plasticity of human adipose lineage cells toward endothelial cells: physiological and therapeutic perspectives. *Circulation.* 2004;109:656–663.
12. Imanishi Y, Saito A, Komoda H, Kitagawa-Sakakida S, Miyagawa S, Kondoh H, Ichikawa H, Sawa Y. Allogenic mesenchymal stem cell transplantation has a therapeutic effect in acute myocardial infarction in rats. *J Mol Cell Cardiol.* 2008;44:662–671.
13. R Development Core Team. R: A language and environment for statistical computing. 2008. R Foundation for Statistical Computing; Vienna, Austria. ISBN 3-900051-07-0. http://www.R-project.org. Accessed August 3, 2011.
14. Kondo K, Shibata R, Unno K, Shimano M, Ishii M, Kito T, Shintani S, Walsh K, Ouchi N, Murohara T. Impact of a single intracoronary administration of adiponectin on myocardial ischemia/reperfusion injury in a pig model. *Circ Cardiovasc Interv.* 2010;3:166–173.
15. Davis ME, Hsieh PC, Grodzinsky AJ, Lee RT. Custom design of the cardiac microenvironment with biomaterials. *Circ Res.* 2005;97:8–15.
16. Yla-Herttuala S, Martin JF. Cardiovascular gene therapy. *Lancet.* 2000; 355:213–222.
17. Joung YK, Bae JW, Park KD. Controlled release of heparin-binding growth factors using heparin-containing particulate systems for tissue regeneration. *Expert Opin Drug Deliv.* 2008;5:1173–1184.
18. Allison SD. Analysis of initial burst in PLGA microparticles. *Expert Opin Drug Deliv.* 2008;5:615–628.
19. Xia Z, Triffitt JT. A review on macrophage responses to biomaterials. *Biomed Mater.* 2006;1:R1–R9.
20. Golocheikine A, Tiriveedhi V, Angaswamy N, Benshoff N, Sabarinathan R, Mohanakumar T. Cooperative signaling for angiogenesis and neovascularization by VEGF and HGF following islet transplantation. *Transplantation.* 2010;90:725–731.
21. Hopkins TA, Ouchi N, Shibata R, Walsh K. Adiponectin actions in the cardiovascular system. *Cardiovasc Res.* 2007;74:11–18.
22. Ouchi N, Walsh K. Adiponectin as an anti-inflammatory factor. *Clin Chim Acta.* 2007;380:24–30.
23. Shibata R, Sato K, Pimentel DR, Takemura Y, Kihara S, Ohashi K, Funahashi T, Ouchi N, Walsh K. Adiponectin protects against myocardial ischemia-reperfusion injury through AMPK- and COX-2-dependent mechanisms. *Nat Med.* 2005;11:1096–1103.
24. Shibata R, Ouchi N, Ito M, Kihara S, Shiojima I, Pimentel DR, Kumada M, Sato K, Schiekofer S, Ohashi K, Funahashi T, Colucci WS, Walsh K. Adiponectin-mediated modulation of hypertrophic signals in the heart. *Nat Med.* 2004;10:1384–1389.
25. Tateno K, Minamino T, Toko H, Akazawa H, Shimizu N, Takeda S, Kunieda T, Miyauchi H, Oyama T, Takeda S, Kunieda T, Miyauchi H, Oyama T, Matsuura K, Nishi J-i, Kobayashi Y, Nagai T, Kuwabara Y, Iwakura Y, Nomura F, Saito Y, Komuro I. Critical roles of muscle-secreted angiogenic factors in therapeutic neovascularization. *Circ Res.* 2006;98:1194.

SUPPLEMENTAL MATERIALS

MS ID#: CIRCULATIONAHA/2010/009993/R1

MS TITLE: Induced Adipocyte Cell-Sheet Ameliorates Cardiac Dysfunction in Mouse Myocardial Infarction Model - A Novel Drug Delivery System for Heart Failure

Materials and Methods

Preparation of Adipocyte cell-sheet

Stromal-vascular fraction (SVF) cells were enzymatically isolated from adipose tissues.[1] Briefly, inguinal adipose tissue was excised from wild type mice (WT; male C57BL/6J), APN knockout (KO) mice which were generated and backcrossed to C57BL/6J over 6 generations as described previously[2], or from rats (3-week-old, male LEW/Sea). Adipose tissue was digested in Hank's balanced buffered saline (Sigma-Aldrich, MO, USA) containing 0.1% collagenase type II (Life Technologies, CA, USA) at 37°C with shaking vigorously for 1 hour. The adipose cell extracts were passed 100 μm and 70 μm filters, resuspended in Dulbecco's Modified Eagle's Medium (Life Technologies) containing 10% fetal bovine serum (Equitech-bio, TX, USA), 200 μM ascorbic acid (Sigma-Aldrich), and antibiotics (Life Technologies), then cultured on culture dishes (AGC Techno Glass, Chiba, Japan) at 37°C and 5% CO_2. Twenty-four hours after plating, all the non-adherent cells were removed by washing. The SVF cells were cultured for 3 days in